New insights into hadron production mechanism from p_T spectra in pp collisions at $\sqrt{s} = 7$ TeV

Xing-rui Gou,[1] Feng-lan Shao,[1,*] Rui-qin Wang,[1] Hai-hong Li,[1,2] and Jun Song[2,†]

[1]*School of Physics and Engineering, Qufu Normal University, Shandong 273165, China*
[2]*Department of Physics, Jining University, Shandong 273155, China*

We show that the experimental data of midrapidity p_T spectra for p, Λ, Ξ, Ω^-, $K(892)^{*0}$, and $\Xi(1530)^{*0}$ in minimum-bias pp collisions at $\sqrt{s} = 7$ TeV can be well fitted by the quark combination mechanism with the parametrized up(down) quark spectrum and strange quark spectrum at hadronization. The averaged transverse momentum $\langle p_T \rangle$ and spectrum ratios such as Ξ/Λ and Ω/ϕ calculated from quark combination reproduce the data quite well. The available data of hadronic p_T spectra released by ALICE collaboration in the first three high-multiplicity classes of pp collisions at $\sqrt{s} = 7$ TeV are also well fitted. The extracted quark spectra at hadronization exhibit a dependence on the multiplicity class and also show a certain similarity to those obtained in p-Pb collisions at LHC and in relativistic heavy ion collisions. We make predictions for other hadrons, and propose two scaling behaviors among decuplet baryons and vector mesons as the effective probe of hadron production mechanism at such high collision energies.

I. INTRODUCTION

At sufficiently high temperature and energy density, nuclear matter undergoes a transition to a phase in which quarks and gluons are not confined: the quark–gluon plasma (QGP) [1]. This deconfined state is usually believed to be formed (with volume of thousand cubic fermi) in ultrarelativistic heavy ion collisions. Unexpectedly, recent ALICE and CMS experiments at Large Hadron Collider (LHC) have revealed a series of interesting properties of hadron production in high multiplicity events of pp and p-Pb collisions, e.g., long range angular correlations [2,3] and collectivity [4–6], enhanced strangeness [7,8] and enhanced baryon to meson ratios at soft transverse momentum [9,10], which in heavy ion collisions are typically attributed to the formation of a strongly interacting QGP. Remarkable similarities in pp, p-Pb and Pb-Pb collisions at LHC have invoked intensive discussions in literature involving the mini-QGP or phase transition [11–16], multiple parton interaction (MPI) [17], string overlap and color reconnection at hadronization [18–21], etc., in the small system created in pp and p-Pb collisions. The search of other new features of hadron production is important to gain deep insights into the property and hadronization of the partonic systems created in pp and p-Pb collisions at LHC.

A series of measurements of transverse momentum p_T spectra of identified hadrons have been carried out and high-precision data have been released by ALICE and CMS collaborations [9,10,22–27]. It is of particular interest to see that these data show any regularities that may lead to deeper insights. In the latest work [28], we found that the data of p_T spectra of identified hadrons in p-Pb collisions at $\sqrt{s_{NN}} = 5.02$ TeV [7,9,10,26,27] released by ALICE collaboration exhibit a striking quark number scaling. This scaling property is a direct consequence of quark (re) combination mechanism (QCM) at hadronization [29–34], and it indicates the constituent quark degrees of freedom play an important rule in hadron production of small systems produced at LHC energies. We surprisingly found that quark number scaling seems to also hold in 40–60% and 60–80% multiplicity classes of p-Pb collisions where the charged-particle multiplicity density at mid-rapidity is relatively small, i.e., $\langle dN_{ch}/d\eta \rangle \sim 10$–20. Considering that $\langle dN_{ch}/d\eta \rangle$ in high-multiplicity events of pp collisions at $\sqrt{s} = 7$ TeV also reach such values and the hadron production in there also exhibits remarkable similarities with those in p-Pb collisions at $\sqrt{s_{NN}} = 5.02$ TeV [2–6], we therefore further study in this paper whether quark combination also works in pp collisions at $\sqrt{s} = 7$ TeV or not.

The paper is organized as follows: Sec. II introduces a working model under quark (re)combination mechanism. Section III and Sec. IV present our results and relevant discussions in minimum-bias events and high-multiplicity events, respectively. Section V present the discussions on the quark number scaling property for p_T spectra of vector mesons and decuplet baryons. A summary is given at last in Sec. VI.

II. HADRON YIELDS AND p_T SPECTRA IN QCM

The application of QCM to the production of hadrons in high energy reactions has a long history [29,30]. QCM describes the formation of hadrons at hadronization by the

*shaofl@mail.sdu.edu.cn
†songjun2011@jnxy.edu.cn

094010-1

combination of quarks and antiquarks neighboring in phase space. The mechanism assumes the effective absence of soft gluon quanta at hadronization and the effective degrees of freedom of QCD matter are only quarks and antiquarks. A quark and an antiquark neighboring in phase space form a meson and three quarks (antiquarks) form a baryon (antibaryon). Relativistic heavy-ion collisions produce a large volume of deconfined quark matter and this makes QCM to be a natural scenario for hadronization [31–41].

The high multiplicity events of pp and p-Pb collisions at LHC show remarkable similarities with those of Pb-Pb collisions [2,3,6–8]. The origin of such similarity is possibly attributed to the formation of dense parton system [11–16] in terms of string overlap or percolation and MPI [17–21], etc. If such dense system is in a QGP-like deconfined state, we prefer to apply QCM to explain the data of pp and p-Pb collisions. In addition, the effects of hadronic re-scatterings are expected to be small for such small systems, and therefore we can get more direct information on the property of the created partonic system and its hadronization.

When we apply QCM to the small parton system, in principle, we should follow, e.g., procedures in Refs. [42,43] by starting from the partons after perturbative evolution to study how to treat them or evolve them in the subsequent nonperturbative stage as a collection of constituent quarks and antiquarks, and finally study how to recombine them into different identified hadrons. However, the current understanding on the multiparton system produced at such high collisions energies is still incomplete, in particular, for high-multiplicity events. Therefore, in this paper we only test the basic characteristics of QCM in pp collisions at $\sqrt{s} = 7$ TeV, that is, we formulate the p_T spectra of hadrons based on a quark statistic method with the effective constituent quark degrees of freedom.

A. Formalism of quark combination in momentum space

In general, for a baryon B_j composed of $q_1 q_2 q_3$ and a meson M_j composed of $q_1 \bar{q}_2$, as formulated in, e.g., [39] we have in QCM

$$f_{B_j}(p_B) = \int dp_1 dp_2 dp_3 \mathcal{R}_{B_j}(p_1, p_2, p_3; p_B)$$
$$\times f_{q_1 q_2 q_3}(p_1, p_2, p_3), \qquad (1)$$

$$f_{M_j}(p_M) = \int dp_1 dp_2 \mathcal{R}_{M_j}(p_1, p_2; p_M) f_{q_1 \bar{q}_2}(p_1, p_2). \qquad (2)$$

Here, $f_{q_1 q_2 q_3}(p_1, p_2, p_3)$ is the joint momentum distribution for q_1, q_2 and q_3. $\mathcal{R}_{B_j}(p_1, p_2, p_3; p_B)$ is the combination function that is the probability for a given $q_1 q_2 q_3$ with momenta p_1, p_2 and p_3 to combine into a baryon B_j with momentum p_B. It is similar for mesons. If we assume

independent distributions of quarks and/or antiquarks, we have

$$f_{q_1 q_2 q_3}(p_1, p_2, p_3) = N_{q_1 q_2 q_3} f_{q_1}^{(n)}(p_1) f_{q_2}^{(n)}(p_2) f_{q_3}^{(n)}(p_3), \qquad (3)$$

$$f_{q_1 \bar{q}_2}(p_1, p_2) = N_{q_1 \bar{q}_2} f_{q_1}^{(n)}(p_1) f_{\bar{q}_2}^{(n)}(p_2). \qquad (4)$$

Here $f_q^{(n)}(p)$ is the single quark distribution with normalization $\int dp f_q^{(n)}(p) = 1$ and the number of quarks of flavor q_i is denoted by N_{q_i}. $N_{q_1 \bar{q}_2} = N_{q_1} N_{\bar{q}_2}$ is the number of possible $q_1 \bar{q}_2$ pairs. $N_{q_1 q_2 q_3} = \int dp_1 dp_2 dp_3 f_{q_1 q_2 q_3}(p_1, p_2, p_3)$ is the number of three quark combinations and takes to be $6 N_{q_1} N_{q_2} N_{q_3}$, $3 N_{q_1}(N_{q_1} - 1) N_{q_2}$ and $N_{q_1}(N_{q_1} - 1)(N_{q_1} - 2)$ for cases of three different flavors, two identical flavors and three identical flavors, respectively. Factors 6 and 3 are numbers of permutations for $q_1 q_2 q_3$ and $q_1 q_1 q_2$ combinations, respectively. We emphasize that the form of $N_{q_1 q_2 q_3}$ has consider some necessary threshold effects for identified hadrons. For example, in Ω^- formation $N_{sss} = N_s(N_s - 1)(N_s - 2)$ means that Ω^- can be only produced in events with strange quark number $N_s \geq 3$.

Suppose the combination takes place mainly for quark and/or antiquark that takes a given fraction of momentum of the hadron, we write the combination function

$$\mathcal{R}_{B_j}(p_1, p_2, p_3; p_B) = \kappa_{B_j} \prod_{i=1}^{3} \delta(p_i - x_i p_B), \qquad (5)$$

$$\mathcal{R}_{M_j}(p_1, p_2; p_M) = \kappa_{M_j} \prod_{i=1}^{2} \delta(p_i - x_i p_M). \qquad (6)$$

Inspired by the latest work in p-Pb collisions at LHC [28], we adopt the approximation of equal transverse velocity in combination, or called co-moving approximation, since we apply the concept of constituent quark structure of hadrons. We recall the velocity is $v = p/E = p/\gamma m$. Equal velocity implies $p_i = \gamma v m_i \propto m_i$ which leads to

$$x_i = m_i / \sum_j m_j, \qquad (7)$$

where quark masses are taken to be the constituent mass $m_s = 500$ MeV and $m_u = m_d = 330$ MeV so that the mass and momentum of hadron can be consistently generated by the combination of these constituent quarks and antiquarks neighboring in momentum space.

Inserting Eqs. (3)–(4) and (5)–(6), we obtain

$$f_{B_j}(p_B) = N_{q_1 q_2 q_3} \kappa_{B_j} f_{q_1}^{(n)}(x_1 p_B) f_{q_2}^{(n)}(x_2 p_B) f_{q_3}^{(n)}(x_3 p_B), \qquad (8)$$

$$f_{M_j}(p_M) = N_{q_1\bar{q}_2}\kappa_{M_j}f_{q_1}(x_1 p_M)f_{\bar{q}_2}(x_2 p_M). \qquad (9)$$

By defining the normalized hadron distributions, for $B_j(q_1 q_2 q_3)$

$$f_{B_j}^{(n)}(p_B) = A_{B_j}f_{q_1}^{(n)}(x_1 p_B)f_{q_2}^{(n)}(x_2 p_B)f_{q_3}^{(n)}(x_3 p_B), \qquad (10)$$

and for $M_j(q_1\bar{q}_2)$

$$f_{M_j}^{(n)}(p_M) = A_{M_j}f_{q_1}^{(n)}(x_1 p_M)f_{\bar{q}_2}^{(n)}(x_2 p_M), \qquad (11)$$

where $A_{B_j}^{-1} = \int \mathrm{d}p \prod_{i=1}^{3} f_{q_i}^{(n)}(x_i p)$ and $A_{M_j}^{-1} = \int \mathrm{d}p f_{q_1}^{(n)}(x_1 p)$ $f_{\bar{q}_2}^{(n)}(x_2 p)$, we finally obtain the following formula of hadronic spectra

$$f_{B_j}(p_B) = N_{B_j}f_{B_j}^{(n)}(p_B), \qquad (12)$$

$$f_{M_j}(p_M) = N_{M_j}f_{M_j}^{(n)}(p_M), \qquad (13)$$

where yields of baryon and meson

$$N_{B_j} = N_{q_1 q_2 q_3}P_{q_1 q_2 q_3 \to B_j} = N_{q_1 q_2 q_3}\frac{\kappa_{B_j}}{A_{B_j}}, \qquad (14)$$

$$N_{M_j} = N_{q_1\bar{q}_2}P_{q_1\bar{q}_2 \to M_j} = N_{q_1\bar{q}_2}\frac{\kappa_{M_j}}{A_{M_j}}. \qquad (15)$$

We see that κ_{B_j}/A_{B_j} is nothing but the momentum-integrated probability of $q_1 q_2 q_3 \to B_j$ and κ_{M_j}/A_{M_j} is the probability of $q_1\bar{q}_2 \to M_j$. If we take the approximation that the probability for $q\bar{q}$ to form a meson and a qqq to form a baryon is flavor independent, the combination probability can be determined with a few parameters

$$P_{q_1 q_2 q_3 \to B_j} = C_{B_j}\frac{\overline{N}_B}{N_{qqq}}, \qquad (16)$$

$$P_{q_1\bar{q}_2 \to M_j} = C_{M_j}\frac{\overline{N}_M}{N_{q\bar{q}}}, \qquad (17)$$

where $\overline{N}_B/N_{qqq}$ denotes the average probability of three quarks combining into a baryon and C_{B_j} is the branch ratio to B_j for a given flavor $q_1 q_2 q_3$ combination. $\overline{N}_B = \sum_j N_{B_j}$ is the average number of total baryons and $N_{qqq} = N_q(N_q - 1)(N_q - 2)$ is the total possible number of three quark combinations for baryon formation. $N_q = \sum_{q_i} N_{q_i}$ is the total quark number. Similarly, $\overline{N}_M/N_{q\bar{q}}$ is used to approximately denote the average probability of a quark and antiquark combining into a meson and C_{M_j} is the branch ratio to M_j for a given flavor $q_1\bar{q}_2$ combination. $\overline{N}_M = \sum_j N_{M_j}$ is total mesons and $N_{q\bar{q}} = N_q N_{\bar{q}}$ is the total

possible number of quark antiquark pairs for meson formation.

Here we consider only the ground state $J^P = 0^-, 1^-$ mesons and $J^P = (1/2)^+, (3/2)^+$ baryons in flavor SU(3) group. For mesons

$$C_{M_j} = \begin{cases} \frac{1}{1+R_{V/P}} & \text{for } J^P = 0^-\text{mesons} \\ \frac{R_{V/P}}{1+R_{V/P}} & \text{for } J^P = 1^-\text{mesons,} \end{cases} \qquad (18)$$

where the parameter $R_{V/P}$ represents the ratio of the $J^P = 1^-$ vector mesons to the $J^P = 0^-$ pseudoscalar mesons of the same flavor composition. For baryons

$$C_{B_j} = \begin{cases} \frac{R_{O/D}}{1+R_{O/D}} & \text{for } J^P = (1/2)^+\text{baryons} \\ \frac{1}{1+R_{O/D}} & \text{for } J^P = (3/2)^+\text{baryons,} \end{cases} \qquad (19)$$

except that $C_\Lambda = C_{\Sigma^0} = R_{O/D}/(1 + 2R_{O/D}), C_{\Sigma^{*0}} = 1/(1 + 2R_{O/D}), C_{\Delta^{++}} = C_{\Delta^-} = C_{\Omega^-} = 1$. Here, $R_{O/D}$ stands for the ratio of the $J^P = (1/2)^+$ octet to the $J^P = (3/2)^+$ decuplet baryons of the same flavor composition. Here, $R_{V/P}$ and $R_{O/D}$ are set to be 0.45 and 2.5, respectively, which are slightly different from Ref. [44], in order to better tune the yields of vector mesons and decuplet baryons. The fraction of baryons relative to mesons is $\overline{N}_B/\overline{N}_M \approx 0.085$ [38,44]. Using the unitarity constraint of hadronization $\overline{N}_M + 3\overline{N}_B = N_q$, N_{B_j} and N_{M_j} can be calculated at given quark numbers at hadronization.

B. Parametrizations of quark number and momentum distribution

The numbers and momentum distributions of constituent quarks and antiquarks at hadronization are the consequence of early perturbative process and subsequent nonperturbative QCD evolution. They cannot be obtained by first-principle QCD calculations at present and therefore have to be parametrized and be treated as the inputs of the model.

For the small quark system created in pp collisions, both the average values of quark numbers and quark number distributions are important in calculation of hadronic yield. A rough estimation from the yield data of single-strangeness hadrons kaon and Λ in minimum-bias pp collisions at $\sqrt{s} = 7$ TeV [8,22] gives that the average number of strange quarks in the unit rapidity interval is only about 0.8. Since the formation of multistrangeness hyperons such as Ω^- (or Ξ) is possible only for events with $N_s \geq 3$ (or 2), yields of those hyperons will be strongly dependent on the fluctuation property of strange quark number. We get the event-averaged hadron yield by

$$\langle N_{h_j}\rangle = \sum_{\{N_{q_i},N_{\bar{q}_i}\}} \mathcal{P}(\{N_{q_i},N_{\bar{q}_i}\}; \{\langle N_{q_i}\rangle, \langle N_{\bar{q}_i}\rangle\})N_{h_j}, \qquad (20)$$

where $\mathcal{P}(\{N_{q_i}, N_{\bar{q}_i}\}; \{\langle N_{q_i}\rangle, \langle N_{\bar{q}_i}\rangle\})$ is the distribution of quark numbers and antiquark numbers. In this paper, we suppose the independent distribution for each flavor of quarks and antiquarks, i.e., $\mathcal{P}(\{N_{q_i}, N_{\bar{q}_i}\}; \{\langle N_{q_i}\rangle, \langle N_{\bar{q}_i}\rangle\}) = \prod_{q_i} \mathcal{P}(N_{q_i}, \langle N_{q_i}\rangle)$. For quark number distribution $\mathcal{P}(N_{q_i}, \langle N_{q_i}\rangle)$ of specific flavor q_i, we firstly adopt the Poisson distribution $\text{Pois}(N_{q_i}; \langle N_{q_i}\rangle)$ as a reference shape for quark number and then introduce a suppression parameter $\gamma_{q_i} \leq 1$ for the long tail of Poisson distribution through a piecewise function $\Theta(N_{q_i}) = \{\{1, N_{q_i} < 3\}, \{\gamma_{q_i}, N_{q_i} \geq 3\}\}$. The practical distribution is $\mathcal{P}(N_{q_i}; \langle N_{q_i}\rangle) = \mathcal{N}\text{Pois}(N_{q_i}; \mu)\Theta(N_{q_i})$ where $\mathcal{N}$ is the normalization factor and μ is solved by the average constraint $\sum_{N_{q_i}} P(N_{q_i}; \langle N_{q_i}\rangle)N_{q_i} = \langle N_{q_i}\rangle$ for given γ_{q_i}. We take $\gamma_u = \gamma_d = 1$ for up and down quarks and take $\gamma_s = 0.6$ for strange quark (antiquark) according to the study of the yields of multistrangeness hyperons in low-multiplicity classes of p-Pb collisions at $\sqrt{s_{NN}} = 5.02$ TeV [44]. The average quark numbers $\langle N_u\rangle = \langle N_d\rangle$ and $\langle N_s\rangle$ are determined by fitting the data of yields of kaon and proton in the studied multiplicity class. The numbers of antiquarks are taken to be the same as those of quarks.

For the p_T distributions of quarks at midrapidity, inspired by the Lévy-Tsallis parametrization [45] for the data of hadronic p_T spectra, we use the following form to parametrize the p_T distribution for quarks

$$f_q^{(n)}(p_T) = \mathcal{N}_q(p_T + a_q)^{b_q}\left(1 + \frac{\sqrt{p_T^2 + m_q^2} - m_q}{n_q c_q}\right)^{-n_q},$$

(21)

where $\mathcal{N}_q$ is the normalization constant satisfying $\int dp_T f_q^{(n)}(p_T) = 1$. Parameter a_q is introduced to tune the spectrum at very small p_T and is taken to be 0.06 GeV. Parameters b_q, n_q and c_q (GeV) tune the behavior of the spectrum at low and intermediate p_T. Considering the isospin symmetry, we take $b_u = b_d$, $n_u = n_d$, and $c_u = c_d$ and therefore $f_u^{(n)}(p_T) = f_d^{(n)}(p_T)$. The values of two parameter group (b_u, n_u, c_u) and (b_s, n_s, c_s) are determined by fitting the data of p_T spectrum a light hadron such as proton and those of a strange hadron such as Ω^-, respectively. The values for antiquarks are the same as those of quarks.

III. RESULTS IN MINIMUM-BIAS pp COLLISIONS

The data of midrapidity p_T spectra for pion, kaon, proton, Λ, Ξ, Ω, ϕ, K(892)^{*0}, $\Sigma(1385)^*$, $\Xi(1530)^*$ are all available for minimum-bias events [22–25]. Constraining ourselves to the midrapidity region $y = 0$, we apply the formulas in previous section to the one-dimensional p_T space and study to what extent QCM

feature exhibits in these data. In addition, we note that predictions from the event generators such as PYTHIA on pp collisions at LHC are available. Considering that these event generators adopt the string or cluster fragmentation to describe the hadronization, we also compare our results with those of event generators to indicate the effects of the possible change of hadronization characteristic in small system created in pp collisions at LHC.

A. Midrapidity p_T spectra of identified hadrons

By fitting the experimental data of mid-rapidity p_T spectra of proton and Ω^- in minimum-bias pp collisions at $\sqrt{s} = 7$ TeV [22,23], we fix parameters for p_T spectra of u quarks and s quarks at hadronization. The $\langle N_u\rangle$ and $\langle N_s\rangle$ in $|y| < 0.5$ interval are taken to be 2.5 and 0.8, respectively. Parameters (b_q, n_q, c_q) of spectrum shape are taken to be $(0.485, 3.93, 0.28)$ for u quarks and $(0.485, 4.05, 0.362)$ for s quarks, respectively. p_T spectra of Λ, Ξ^0, ϕ, K(892)^{*0}, $\Xi(1530)^{*0}$, and $\Sigma(1385)^{*+}$ are then calculated. Figure 1 presents the results of QCM (shown as solid lines) and compares them with experimental data [22–25,46] shown as symbols. Decuplet baryons Ω^-, Ξ^*, Σ^* and vector mesons K(892)^{*0} and ϕ are less influenced by decay, and, therefore, behaviors of these hadrons are usually believed as carrying more direct information from hadronization. We see that the spectrum shape of Ω^-, Ξ^*, $\Sigma^*(1385)$, and K(892)^{*0} are simultaneously well described. Result of ϕ is somewhat flatter than the data. Results of proton, Λ, Ξ^0 that further take decay influence into account are also in good agreement in spectrum shapes with the experimental data. Because the masses of pion and kaon are significantly smaller than the summed masses of their constituent (anti-)quarks, data of pion and kaon are not suitable to directly test the QCM as the above hadrons, and their results are discussed in Appendix A.

To further quantify our results, we calculate the yield at mid rapidity $N_h = \int f_h(p_T)dp_T$ and average transverse momentum $\langle p_T\rangle = N_h^{-1} \int p_T f_h(p_T)dp_T$, and show them in Table I and compare with the available experimental data. For yields, we see that on the whole our results are in good agreement with the data. In particular, the hierarchy property among yields of p, Λ, Ξ^0, Ξ^{*0}, Ω^- which span three orders of magnitude is well reproduced. For hadronic $\langle p_T\rangle$, we get a better agreement with the data considering the statistical and systematical uncertainties.

B. Discussions on $\langle p_T\rangle$ and particle ratios

In Fig. 2, we show the ratio of data of $\langle p_T\rangle$ to our results for different identified hadrons, and compare them with results from different models or event generators. We see that the deviation of our results from the data is in general less than about 5%. Popular event generator PYTHIA [47] adopts the string fragmentation [48] for hadronization. Results from PYTHIA6 P2011 (tune Perugia2011) [49], solid
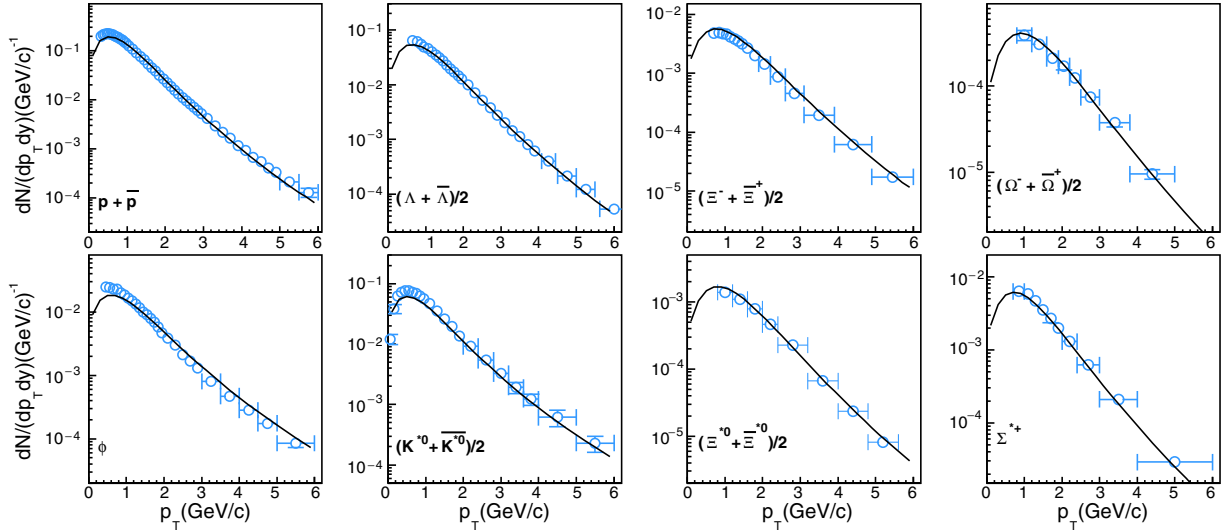
FIG. 1. Midrapidity p_T spectra of identified hadrons in minimum-bias pp collisions at $\sqrt{s} = 7$ TeV. The solid lines are QCM results and symbols are experimental data [22–25].

circles, show that it predicts the much soft p_T spectra for multi-strangeness hadrons, i.e., about 20% softer than the data. Taking effects of color re-connection into account seems to little change the $\langle p_T \rangle$ results [21]. Recently, a new model of generating the transverse momentum of hadrons during the string fragmentation process, inspired by thermodynamics, can improve $\langle p_T \rangle$ results of multi-strangeness hyperons with degrees of about 5% [50]. In addition, PYTHIA usually under-estimates yields of multi-strangeness hadrons Ξ and Ω^-, which however can be relieved by color re-connection [20,21,51] and/or string overlap effects realized in DIPSY [19]. Popular event generator SHERPA adopts the cluster fragmentation [52] for hadronization. It also predicts too soft spectra for multi-strangeness hadrons with about 15% deviations.

In Fig. 3, we show the result of $(\Omega^- + \bar{\Omega}^+)$ to $(\Xi^- + \bar{\Xi}^+)$ ratio as a function of $m_T - m_0$ in minimum-bias pp collisions at $\sqrt{s} = 7$ TeV, and compare it with the

TABLE I. Yield densities and average transverse momentum $\langle p_T \rangle$ in minimum-bias pp collisions at $\sqrt{s} = 7$ TeV. Experimental data are from [22–25,46].

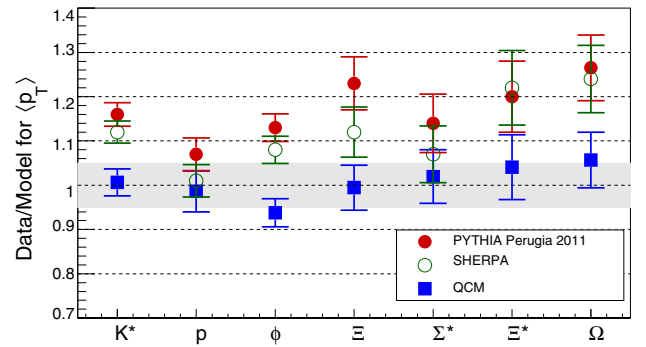|	$\frac{dN}{dy}(\times 10^2)$		$\langle p_T \rangle$	
	Data	QCM	Data	QCM
K^{*0}	$9.7 \pm 0.04^{+1.0}_{-0.9}$	8.4	$1.01 \pm 0.003 \pm 0.02$	1.00
ϕ	$3.2 \pm 0.04^{+0.4}_{-0.35}$	2.9	$1.07 \pm 0.005 \pm 0.03$	1.13
p	12.4 ± 0.9	12.1	0.9 ± 0.029	0.91
Λ	8.1 ± 1.5	7.7	$1.037 \pm 0.005 \pm 0.063$	1.05
Ξ^0	$0.79 \pm 0.01^{+0.07}_{-0.05}$	0.91	$1.21 \pm 0.01 \pm 0.06$	1.215
Σ^{*+}	$1.0 \pm 0.02^{+0.15}_{-0.14}$	0.94	$1.16 \pm 0.02 \pm 0.07$	1.14
Ξ^{*0}	$0.256 \pm 0.007^{+0.040}_{-0.037}$	0.28	$1.31 \pm 0.02 \pm 0.09$	1.26
Ω^-	$0.0675 \pm 0.003^{+0.008}_{-0.006}$	0.075	$1.455 \pm 0.03 \pm 0.08$	1.38

FIG. 2. The ratios of average transverse momentum $\langle p_T \rangle$ for experimental data to those for models or event generators in minimum-bias pp collisions at $\sqrt{s} = 7$ TeV [22–25].
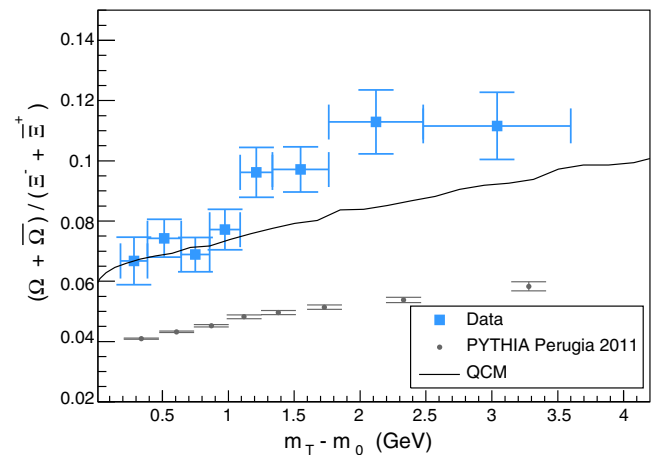

FIG. 3. $(\Omega^- + \bar{\Omega}^+)$ to $(\Xi^- + \bar{\Xi}^+)$ ratio as a function of $m_T - m_0$ in minimum-bias pp collisions at $\sqrt{s} = 7$ TeV. Solid squares are experimental data and solid circles are PYTHIA Perugia 2011 simulation [49], which are taken from [23]. The line is our result.
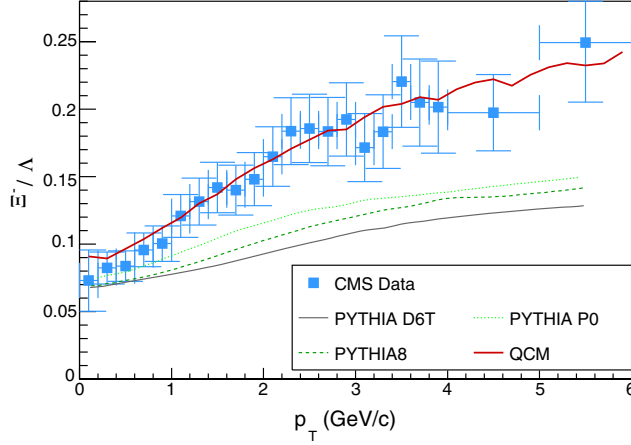
FIG. 4. Ξ^-/Λ ratio as a function of p_T in minimum-bias pp collisions at $\sqrt{s} = 7$ TeV. Solid squares are experimental data from CMS collaboration [46] and thin lines are prediction of different PYTHIA versions and/or tunes [53–55], which are taken from [46]. The thick line is our result.
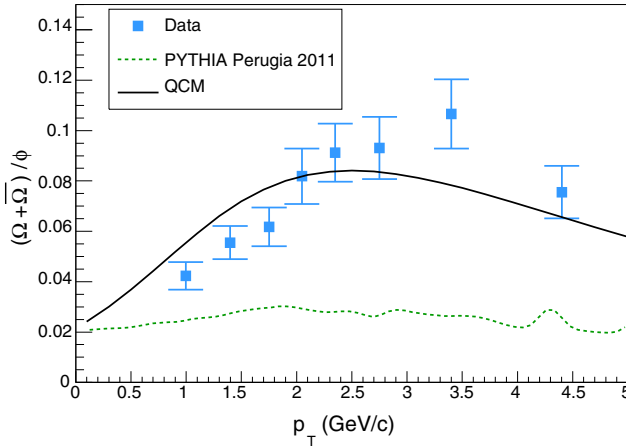

FIG. 5. $(\Omega^- + \bar{\Omega}^+)$ to ϕ ratio as a function of p_T in minimum-bias pp collisions at $\sqrt{s} = 7$ TeV. Solid squares are experimental data; dashed line is PYTHIA Perugia 2011 simulation [49]; they are taken from [24]. The solid line is our result.

data [23]. Our result is consistent with the data at low $m_T - m_0$ and is slightly below the data at moderate $m_T - m_0$ in magnitude. PYTHIA P2011 [49] predicts a too low ratio, but as mentioned above, consideration of color reconnection and string overlap will raise the ratio to a certain extent.

In Fig. 4 we show Ξ^-/Λ ratio as a function of p_T in minimum-bias pp collisions at $\sqrt{s} = 7$ TeV, and compare it with the experimental data from CMS collaboration [46]. Results of PYTHIA6 D6T tune [53], Perugia0 (P0) tune [54], and PYTHIA8 [55] are also shown. We see that our result is in good agreement with the data.

In Fig. 5, we show the result of $(\Omega^- + \bar{\Omega}^+)$ to ϕ ratio as a function of p_T in minimum-bias pp collisions at

$\sqrt{s} = 7$ TeV. Our result is slightly higher than the data at $p_T \lesssim 2$ GeV and is slightly lower than the data for p_T around 3.5 GeV, but on the whole the magnitude and shape are in good agreement with the data [24]. We emphasize that such behavior of baryon/meson ratio is a typical property of QCM and had been observed many times in AA and pA collisions at RHIC and LHC [31–33,36,56]. PYTHIA6 P2011 [49] predicts an obviously low and flat ratio.

In short summary of this section, on the whole we see that the data of hadronic p_T spectra in minimum-bias pp collisions at $\sqrt{s} = 7$ TeV can be well fitted by QCM using a u quark spectrum and a s quark spectrum at hadronization. This indicates that the constituent quark degrees of freedom and their combination dynamics at hadronization are needed for a better understanding of the hadron production in pp collisions at such high energy. In addition, there exists certain deviations for yield and/or p_T spectra of a few hadrons at about 10% level. In particular, we note that p_T spectrum of Ω^- and that of ϕ seems to be hardly reproduced by the same one s quark distribution. This might be because that most events in minimum-bias event collections have small charged particle multiplicities (or quark numbers in QCM language and/or effective energy for particle production in general language). Various kinds of threshold effects may appear for these events. For example, too small s-quark numbers, i.e., $N_s < 3$ (or too small effective energy for s quark production) in an event will inhibit the formation of Ω and/or constrain its carrying momentum. Therefore, we expect that, in high multiplicity events of pp collisions where the number of quarks (or effective energy for particle production) is large and such threshold effects are weak, QCM will make better prediction for the production of identified hadrons.

IV. PREDICTIONS IN HIGH-MULTIPLICITY EVENTS OF pp COLLISIONS

Midrapidity $\langle dN_{ch}/d\eta \rangle$ in first three high-multiplicity classes 0–0.95% (I), 0.95–4.7% (II) and 4.7–9.5% (III) in pp collisions at LHC are 21.3 ± 0.6, 16.5 ± 0.5, and 13.5 ± 0.4 [8]. High multiplicity means the high energy deposited in the collision region by the intense partonic interactions happening in early stage of collisions, which increases the possibility of the formation of the deconfined system. Indeed, the experimental data have shown that production of hadrons in high-multiplicity events in pp collisions exhibit lots of remarkable similarities with p-Pb collisions and Pb+Pb collisions [2,3,6,8]. If QGP-like deconfined system does form in these high-multiplicity collisions, we can apply QCM in a more natural way and expect to make better predictions for the momentum spectra of identified hadrons.

We fix parameters for quark spectra at hadronization in three multiplicity classes by fitting the corresponding data of midrapidity p_T spectra of proton and K(892)*0 [8,57]. The parameter values for spectrum shapes (except

TABLE II. The parameters n_q and c_q for quark p_T spectra, quark numbers $\langle N_u \rangle$ and $\langle N_s \rangle$ in the rapidity interval $|y| \leq 0.5$ in first three multiplicity classes in pp collisions at $\sqrt{s} = 7$ TeV.

Event classes	n_u	c_u (GeV)	n_s	c_s (GeV)	$\langle N_u \rangle$	$\langle N_s \rangle$
Class I	4.45	0.35	5.56	0.46	10.9	3.7
Class II	4.25	0.33	5.26	0.43	8.4	2.8
Class III	4.12	0.31	5.00	0.40	7.2	2.4

$a_q = 0.05$ GeV, $b_q = 0.5$) and quark numbers are shown in Table II. p_T spectra of other hadrons Λ, Ξ^0, ϕ, Ω, $\Xi(1530)^{*0}$, and $\Sigma(1385)^{*+}$ are then calculated. Figure 6 shows results of QCM and compares them with available experimental data [8,57]. The average transverse momenta $\langle p_T \rangle$ are also calculated and are compared with available experimental data [8,58] in Fig. 7.

From Fig. 6, we see that the spectrum shapes of proton, Λ, Ξ, Ω, and $K(892)^{*0}$ are simultaneously well described. Predictions of ϕ, Ξ^*, and Σ^{*+} are presented. Figure 7 shows results of $\langle p_T \rangle$ for proton, Λ and Ξ are in good agreement with the data. The result of ϕ is slightly smaller than the preliminary data [58]. The data of Ω in multiplicity class (I) + (II) are also shown in Fig. 7 as a visual guide. Our result of $\langle p_T \rangle$ for Ω in the average of classes (I) + (II) is 1.57, which is 5% smaller than the data 1.62 ± 0.05 [8]. We note that the behaviors of Ω and ϕ in comparison with data in high multiplicity events are different from those in

minimum-bias events shown in Table I, where the $\langle p_T \rangle$ of Ω is slightly smaller than the data while that of ϕ is larger the data.

In addition, by fitting the data of hadronic p_T spectra, we obtain the p_T spectra of u (or d) quark and s quark at hadronization, which show some interesting properties. First, we see from Table II that both n_q and c_q ($q = u, s$) increase with the increase of charged-particle multiplicity, which means the p_T spectra of quarks become flat and the average p_T becomes large for larger charged-particle multiplicity. This is related to the increased multiple parton interactions with the increased parton system size and/or parton density [18,19,59]. Second, we see that parameter values of strange quarks are different from those of up quarks. As an example, we plot $f_s^{(n)}(p_T)$ and $f_u^{(n)}(p_T)$ in the highest-multiplicity class (I) in Fig. 8. We see that the obtained spectrum for strange quark is flatter than that for u or d quarks for p_T less than 3 GeV. We also plot the ratio between them where we see it raises with p_T and seems to reach the maximum at p_T around 3 GeV. Results in other multiplicity classes and in minimum-bias events are similar. We note that such property is similar to those obtained in p-Pb collisions at $\sqrt{s_{NN}} = 5.02$ TeV [28] and those obtained in heavy ion collisions at RHIC and LHC energies [37,41,60]. This is an indication of some universal property for constituent quarks evolved from the nonperturbative stage. Third, the extracted quark spectra, as shown in Fig. 8,
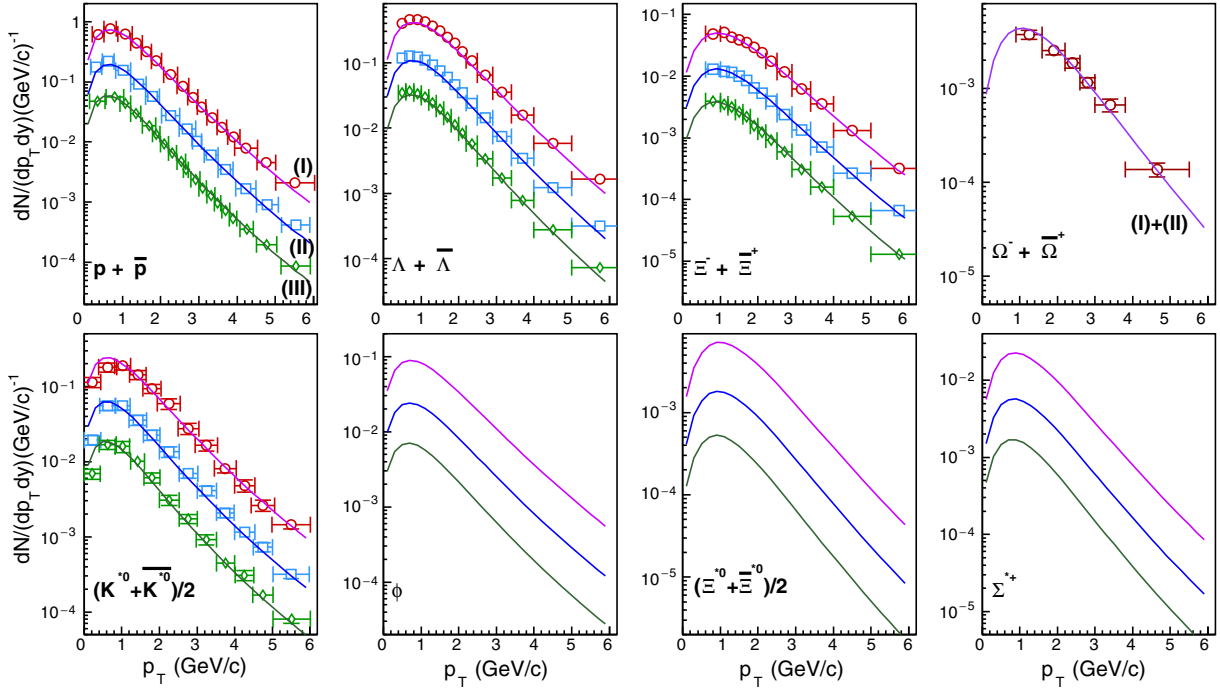

FIG. 6. Midrapidity p_T spectra of identified hadrons in first three high-multiplicity classes (I), (II), (III) in pp collisions at $\sqrt{s} = 7$ TeV. The solid lines are QCM results and symbols are experimental data. The data of Λ, Ξ and Ω^- are from [8] and those of proton and $K(892)^{*0}$ are preliminary [57]. The data and our results in classes (II) and (III) are divided by factors 3 and 3^2 for clarity, respectively.
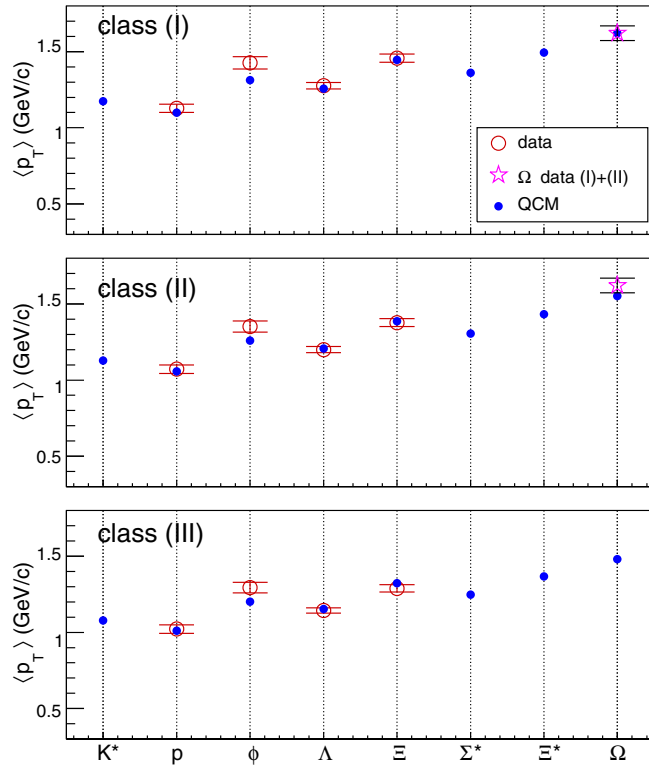
FIG. 7. $\langle p_T \rangle$ of identified hadrons in first three high-multiplicity classes (I), (II), and (III) in pp collisions at $\sqrt{s} = 7$ TeV. Open symbols are experimental data [8,58].
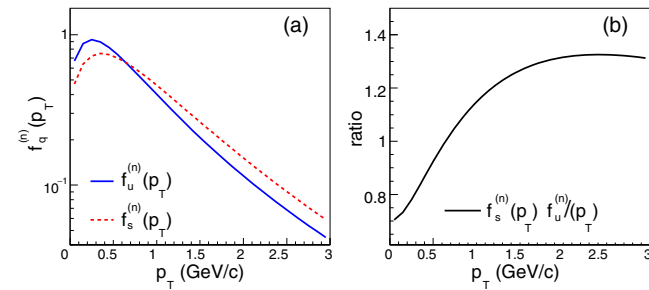

FIG. 8. The p_T spectra of u and s quarks in multiplicity class (I) and the ratio between them.

explicitly deviate from the exponential distribution $dn/(p_T dp_T dy) = \exp(-\sqrt{p_T^2 + m_q^2}/T)$ which usually serves as a characterization of thermal equilibrium. This indicates that the thermal equilibrium may not be reached for the parton system produced in the studied multiplicity classes in pp collisions at $\sqrt{s} = 7$ TeV.

V. DISCUSSIONS ON QUARK NUMBER SCALING OF HADRONIC p_T SPECTRA

If QCM indeed dominates the hadronization process of small partonic system created in pp and p-Pb collisions,

we can obtain several interesting scaling properties for p_T spectra of identified hadron. In particular, for Ω^- and ϕ that are composed of only strange quarks (antiquarks), we have

$$f_\Omega^{1/3}(3p_T) = \kappa_{\phi,\Omega} f_\phi^{1/2}(2p_T), \qquad (22)$$

where $\kappa_{\phi,\Omega}$ is a constant independent of p_T. This is obtained directly from Eqs. (10)–(13) and has been experimentally verified by the data of high-multiplicity p-Pb collisions at $\sqrt{s_{NN}} = 5.02$ TeV [28]. However, we should emphasize that such scaling property only holds under the conditions Eqs. (3) and (4) which are usually valid for a relatively large system. We also expect other scaling behaviors for decuplet baryons such as Ξ^{*0} and vector mesons such as $K(892)^{*0}$, e.g.,

$$\frac{f_{\Xi^{*0}}((2+r)p_T)}{f_{K^{*0}}((1+r)p_T)} = \kappa_{\phi,K^*,\Xi^*} f_\phi^{1/2}(2p_T) \qquad (23)$$

where κ_{ϕ,K^*,Ξ^*} is constant. r denotes the ratio of transverse momentum carried by u or d quark to that of s quark(s), and takes to be about $2/3$ in equal transverse velocity combination if we take $m_s = 500$ MeV and $m_u = m_d = 330$ MeV. It is also experimentally verified by the data of high-multiplicity p-Pb collisions at $\sqrt{s_{NN}} = 5.02$ TeV [28].

We find that the above two scaling properties are broken for the data of minimum-bias pp collisions at $\sqrt{s} = 7$ TeV, as shown in Fig. 9(a). We see that the scaled data $f_\Omega^{1/3}(3p_T)$ is flatter than the scaled data $f_\phi^{1/2}(2p_T)$. This, however, is not an indication for the failure of QCM but is more related to the event mix feature of minimum-bias data set. As we know, only in events with $N_s \geq 3$ both Ω^- and ϕ can be potentially formed and in other events only ϕ can be formed. In general, more strange quarks produced in an event means the more intensive partonic interactions that will broaden transverse momenta, which can be inferred from the increases of $\langle p_T \rangle$ as the function of $\langle dN_{ch}/d\eta \rangle$ [58]. Therefore it is reasonable to expect that the $f_s(p_T)$ in events $N_s \geq 3$ for Ω^- formation is broader than that in events $N_s \geq 1$ for ϕ formation, which leads the observation in Fig. 9(a). Because of similar reasons, the scaled data f_{Ξ^*}/f_{K^*} is also flatter than the scaled data $f_\phi^{1/2}(2p_T)$.

By selecting the high-multiplicity events where the strange quark number is usually large than 3 and the above threshold effects are negligible, we can expect the restoration of quark number scaling for p_T spectra of hadrons. A rough estimation gives that such events should have quarks and antiquarks with numbers at least $N_s \gtrsim 3$ and $N_u = N_d \gtrsim 9$ at midrapidities, which is corresponding to the events with the produced charged-particle density $dN_{ch}/d\eta \gtrsim 20$. Such $dN_{ch}/d\eta$ is reached in high-multiplicity class (I) in pp collisions at $\sqrt{s} = 7$ TeV. Unfortunately, the data of ϕ, $K(892)^{*0}$ and Ξ^* are unavailable at present to carry out such test. However, we have got
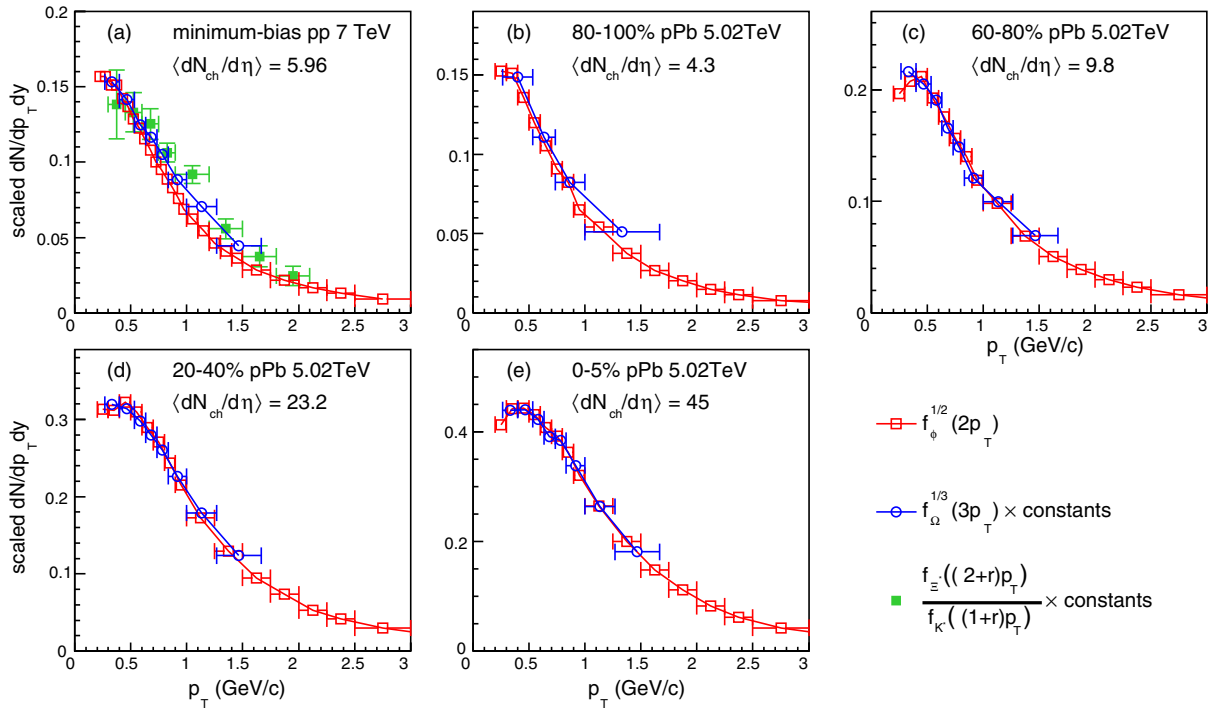
FIG. 9. The scaled data for midrapidity p_T spectra of Ω^- and ϕ in minimum-bias pp collisions at $\sqrt{s} = 7$ TeV [8,24] and those in different multiplicity classes in p-Pb collisions at $\sqrt{s_{NN}} = 5.02$ TeV [7,26].

some hint from the discussions around Fig. 7 in the above section where we find that preliminary data for $\langle p_T \rangle$ of Ω^- and ϕ can be potentially reproduced by the same s-quark p_T distribution. In addition, we may get some indications also from the restoration of quark number scaling for the data of p-Pb collisions at $\sqrt{s_{NN}} = 5.02$ TeV with the increase of the charged-particle multiplicity at midrapidity, which is shown in Figs. 9(b)–9(e).

Some comments on the relation of our works/results and the creation of the deconfined QGP-like system are necessary. Quark combination is a microscopic mechanism for hadronization and in principle it can be applied to various partonic final states created in high energy reactions. In particular, we recall that it was successfully used to explain the hadron production in $e^+ e^-$, pp, $p\bar{p}$, and other hadron reactions in early years, see e.g., Refs. [30,42, 61–63], where the deconfined system is not created. Therefore, the key point on the application of quark combination mechanism to study the formation of deconfined system is that whether we can find some "free" characteristics for the quarks and antiquarks extracted from hadron observables in specific reactions. Equations (22) and (23) are such kinds of examples, which have been observed in high-multiplicity p-Pb collisions at $\sqrt{s_{NN}} = 5.02$ TeV. The observation of Eqs. (22) and (23) indicates that s quark can freely combine with neighboring quarks and/or antiquarks so that it can not only form Ω^- but also form ϕ, K^*, Ξ^* etc. Together with the analysis of charged-particle multiplicity, we finally

obtain that, e.g., in high-multiplicity p-Pb collisions at $\sqrt{s_{NN}} = 5.02$ TeV, there exist a underlying source with dozens of quarks and antiquarks which can freely combine with each other into hadrons at hadronization. We think it is a possible signal for the creation of deconfined system in these collisions.

VI. SUMMARY

We have studied the midrapidity p_T spectra of identified hadrons in pp collisions at $\sqrt{s} = 7$ TeV in the quark combination mechanism for the hadron formation at hadronization. We introduced a working model for the combination of quarks and antiquarks at hadronization with independent momentum distributions under equal velocity combination. The p_T spectra of quarks and antiquarks at hadronization are parametrized as inputs of the model. The experimental data of midrapidity p_T spectra of identified hadrons except ϕ in minimum-bias events can be well fitted by the model using an up quark spectrum and a strange quark spectrum. The hierarchy among yields of proton, Λ, Ξ, and Ω with different strangeness content exhibited in experimental data is well reproduced. The data of the average transverse momentum $\langle p_T \rangle$ are well described with $\lesssim 5\%$ deviations. The ratios of Ω/Ξ, Ξ/Λ, and Ω/ϕ as the function of p_T are well described both in magnitude and shape. In first three classes of high-multiplicity events in pp collisions where the deconfined system is most possibly created, the available data of p_T spectra of hadrons are also

well fitted by the model. These results suggest that the constituent quark degrees of freedom play an important role for hadron production also in such small systems at LHC energy. The extracted p_T spectra of quarks at hadronization in these multiplicity classes are important results, which exhibit a certain dependence on the multiplicity class and also show a certain universal behavior similar to p-Pb collisions at LHC and relativistic heavy ion collisions. We further predicted the p_T distributions of other hadrons for the future test and discussed the possible existence of two interesting scaling behaviors for the p_T spectra of decuplet baryons and vector mesons in high-multiplicity pp collisions at LHC, which have been observed in p-Pb collisions at $\sqrt{s_{NN}} = 5.02$ TeV.

ACKNOWLEDGMENTS

APPENDIX A: p_T SPECTRA OF PION AND KAON

The mass of a pion is much smaller than the sum of the masses of its constituent quarks if we take $m_u = m_d = 330$ MeV. There is a large energy discrepancy in direct combination $u(d) + \bar{u}(\bar{d}) \to \pi$. Similar situation occurs for pseudoscalar kaon in $u(d) + \bar{s} \to K$ or $\bar{u}(\bar{d}) + s \to \bar{K}$ process with $m_s = 500$ MeV and the above m_u and m_d.

A possible phenomenological solution to this issue is that we consider

$$u + \bar{d} \to \pi^+ + X, \tag{A1}$$

$$u + \bar{s} \to K^+ + X, \tag{A2}$$

where X is some soft degrees of freedom at hadronization. The energy conservation is satisfied explicitly in this way. X may be identified as neutral pion and the reaction is a two to two process. X may also be identified as soft gluons which could be absorbed in formation process of other hadrons with large masses. We consider the kinetic influence of such uncertainties on p_T spectra of pion and kaon by setting $0 \lesssim m_X \leq m_\pi$. For $u + \bar{u} \to R$ combination, we consider its two possible outgoing channels $\pi^0 + \pi^0$ and $\pi^+ + \pi^-$ with equal weight.

In Fig. 10(a), we show results of p_T spectra of kaon and pion obtained this way in minimum-bias pp collisions at $\sqrt{s} = 7$ TeV, in which the decay contribution from other hadrons is also included. We find that the result of pion changes little for $0 < m_X \leq m_\pi$, which is mainly because most of pions observed in experiments are from the decay of other hadrons. Our result of pion is found to be in good
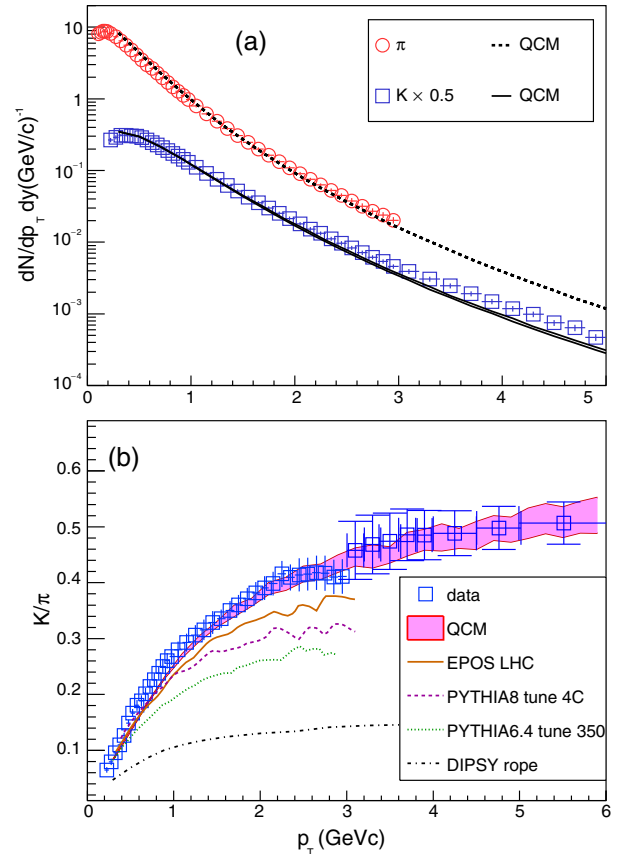

FIG. 10. Midrapidity p_T spectra of kaon and pion in minimum-bias pp collisions at $\sqrt{s} = 7$ TeV and the ratio between them. Symbols are experimental data [22,58] and results of other models and/or event generators are taken from [22,51].

agreement with the available experimental data. The result of kaon changes weakly for $0 < m_X \leq m_\pi$, which is shown as a very thin band in the calculated p_T spectrum for kaon in Fig. 10(a). We see that the result is in good agreement with the data of kaon for $p_T \lesssim 2$ GeV but is lower than the data to a certain extent at moderate p_T, which may show some limitation of such a crude treatment for kaon formation in Eq. (A2) and perhaps for pion in Eq. (A1) also.

In Fig. 10(b), we show the ratio of kaon to pion as the function of p_T which may cancel such limitation to a certain extent. The ratio is dependent on m_X to a certain extent as $p_T \gtrsim 1.5$ GeV and therefore is shown as a band corresponding to $0 < m_X \leq m_\pi$. We find that it agrees well with the experimental data [22,58]. We also show results of PYTHIA with different versions and/or tunes [49,55], DIPSY with string overlap effect by color rope [51], and EPOS for LHC [64] as the characteristics of string fragmentation. Our results for p_T spectra of kaon and pion in high-multiplicity classes (I), (II), and (III) are similar to those in minimum-bias events, and in particular, the K/π ratios are also well explained.

[1] E. V. Shuryak, Quantum chromodynamics and the theory of superdense matter, Phys. Rep. **61**, 71 (1980).

[2] V. Khachatryan *et al.* (CMS Collaboration), Observation of long-range near-side angular correlations in proton-proton collisions at the LHC, J. High Energy Phys. 09 (2010) 091.

[3] S. Chatrchyan *et al.* (CMS Collaboration), Observation of long-range near-side angular correlations in proton-lead collisions at the LHC, Phys. Lett. B **718**, 795 (2013).

[4] V. Khachatryan *et al.* (CMS Collaboration), Evidence for Collective Multiparticle Correlations in p-Pb Collisions, Phys. Rev. Lett. **115**, 012301 (2015).

[5] V. Khachatryan *et al.* (CMS Collaboration), Evidence for collectivity in pp collisions at the LHC, Phys. Lett. B **765**, 193 (2017).

[6] A. Ortiz Velasquez (BNL-Bielefeld-CCNU Collaboration), Production of $\pi/K/p$ from intermediate to high pT in pp, p-b and p-Pb collisions measured by ALICE, Nucl. Phys. **A932**, 146 (2014).

[7] J. Adam *et al.* (ALICE Collaboration), Multi-strange baryon production in p-Pb collisions at $\sqrt{s_{NN}} = 5.02$ TeV, Phys. Lett. B **758**, 389 (2016).

[8] J. Adam *et al.* (ALICE Collaboration), Enhanced production of multi-strange hadrons in high-multiplicity proton-proton collisions, Nat. Phys. **13**, 535 (2017).

[9] B. B. Abelev *et al.* (ALICE Collaboration), Multiplicity dependence of pion, kaon, proton and lambda production in p-Pb collisions at $\sqrt{s_{NN}} = 5.02$ TeV, Phys. Lett. B **728**, 25 (2014).

[10] J. Adam *et al.* (ALICE Collaboration), Multiplicity dependence of charged pion, kaon, and (anti)proton production at large transverse momentum in p-Pb collisions at $\sqrt{s_{NN}} = 5.02$ TeV, Phys. Lett. B **760**, 720 (2016).

[11] F.-M. Liu and K. Werner, Direct Photons at Low Transverse Momentum: A QGP Signal in pp Collisions at LHC, Phys. Rev. Lett. **106**, 242301 (2011).

[12] K. Werner, I. Karpenko, and T Pierog, The 'Ridge' in Proton-Proton Scattering at 7 TeV, Phys. Rev. Lett. **106**, 122004 (2011).

[13] A. Bzdak, B. Schenke, P. Tribedy, and R. Venugopalan, Initial state geometry and the role of hydrodynamics in proton-proton, proton-nucleus and deuteron-nucleus collisions, Phys. Rev. C **87**, 064906 (2013).

[14] P. Bozek and W. Broniowski, Collective dynamics in high-energy proton-nucleus collisions, Phys. Rev. C **88**, 014903 (2013).

[15] S. K. Prasad, V. Roy, S. Chattopadhyay, and A. K. Chaudhuri, Elliptic flow (v_2) in pp collisions at energies available at the CERN Large Hadron Collider: A hydrodynamical approach, Phys. Rev. C **82**, 024909 (2010).

[16] E. Avsar, C. Flensburg, Y. Hatta, J.-Y. Ollitrault, and T. Ueda, Eccentricity and elliptic flow in proton-proton collisions from parton evolution, Phys. Lett. B **702**, 394 (2011).

[17] T. Sjöstrand and M. van Zijl, A multiple interaction model for the event structure in hadron collisions, Phys. Rev. D **36**, 2019 (1987).

[18] I. Bautista, A. F. Téllez, and P. Ghosh, Indication of change of phase in high-multiplicity proton-proton events at LHC in string percolation model, Phys. Rev. D **92**, 071504 (2015).

[19] C. Bierlich, G. Gustafson, L. Lönnblad, and A. Tarasov, Effects of overlapping strings in pp collisions, J. High Energy Phys. 03 (2015) 148.

[20] A. Ortiz Velasquez, P. Christiansen, E. Cuautle Flores, I. Maldonado Cervantes, and G. Paić, Color Reconnection and Flowlike Patterns in pp Collisions, Phys. Rev. Lett. **111**, 042001 (2013).

[21] J. R. Christiansen and P. Z. Skands, String formation beyond leading colour, J. High Energy Phys. 08 (2015) 003.

[22] J. Adam *et al.* (ALICE Collaboration), Measurement of pion, kaon and proton production in proton-proton collisions at $\sqrt{s} = 7$ TeV, Eur. Phys. J. C **75**, 226 (2015).

[23] B. Abelev *et al.* (ALICE Collaboration), Multi-strange baryon production in pp collisions at $\sqrt{s} = 7$ TeV with ALICE, Phys. Lett. B **712**, 309 (2012).

[24] B. Abelev *et al.* (ALICE Collaboration), Production of $K^*(892)^0$ and $\phi(1020)$ in pp collisions at $\sqrt{s} = 7$ TeV, Eur. Phys. J. C **72**, 2183 (2012).

[25] B. B. Abelev *et al.* (ALICE Collaboration), Production of $\Sigma(1385)^\pm$ and $\Xi(1530)^0$ in proton-proton collisions at $\sqrt{s} = 7$ TeV, Eur. Phys. J. C **75**, 1 (2015).

[26] J. Adam *et al.* (ALICE Collaboration), Production of $K^*(892)^0$ and ϕ (1020) in p-Pb collisions at $\sqrt{s_{NN}} = 5.02$ TeV, Eur. Phys. J. C **76**, 245 (2016).

[27] D. Adamova *et al.* (ALICE Collaboration), Production of $\Sigma(1385)^\pm$ and $\Xi(1530)^0$ in p-Pb collisions at $\sqrt{s_{NN}} = 5.02$ TeV, Eur. Phys. J. C **77**, 389 (2017).

[28] J. Song, X.-r. Gou, F.-l. Shao, and Z.-T. Liang, Quark number scaling of hadronic p_T spectra and constituent quark degree of freedom in p-Pb collisions at $\sqrt{s_{NN}} = 5.02$ TeV, Phys. Lett. B **774**, 516 (2017).

[29] J. D. Bjorken and G. R. Farrar, Particle ratios in energetic hadron collisions, Phys. Rev. D **9**, 1449 (1974).

[30] K. P. Das and R. C. Hwa, Quark-antiquark recombination in the fragmentation region, Phys. Lett. **68B**, 459 (1977); Erratum, Phys. Lett. **73B**, 504 (1978).

[31] V. Greco, C. M. Ko, and P. Lévai, Parton Coalescence and Anti-proton/Pion Anomaly at RHIC, Phys. Rev. Lett. **90**, 202302 (2003).

[32] R. J. Fries, B. Müller, C. Nonaka, and S. A. Bass, Hadronization in Heavy Ion Collisions: Recombination and Fragmentation of Partons, Phys. Rev. Lett. **90**, 202303 (2003).

[33] R. C. Hwa and C. B. Yang, Scaling behavior at high p(T) and the p/pi ratio, Phys. Rev. C **67**, 034902 (2003).

[34] F.-l. Shao, Q.-b. Xie, and Q. Wang, Production rates for hadrons, pentaquarks $\Theta+$ and $\Theta*++$, and di-baryon $(\Omega\Omega)_{0+}$ in relativistic heavy ion collisions by a quark combination model, Phys. Rev. C **71**, 044903 (2005).

[35] J. Zimányi, T. S. Biró, T. Csörgő, and P. Lévai, Quark liberation and coalescence at CERN SPS, Phys. Lett. B **472**, 243 (2000).

[36] L.-W. Chen and C. M. Ko, phi and omega production from relativistic heavy ion collisions in a dynamical quark coalescence model, Phys. Rev. C **73**, 044903 (2006).

[37] C.-e. Shao, J. Song, F.-l. Shao, and Q.-b. Xie, Hadron production by quark combination in central Pb+Pb collisions at s(NN)(1/2) = 17.3-GeV, Phys. Rev. C **80**, 014909 (2009).

[38] J. Song and F.-l. Shao, Baryon-antibaryon production asymmetry in relativistic heavy ion collisions, Phys. Rev. C **88**, 027901 (2013).

[39] R.-q. Wang, F.-l. Shao, J. Song, Q.-b. Xie, and Z.-t. Liang, Hadron yield correlation in combination models in high energy AA collisions, Phys. Rev. C **86**, 054906 (2012).

[40] R.-q. Wang, F.-l. Shao, and Z.-t. Liang, Baryon-antibaryon flavor correlation in quark-combination models in heavy-ion collisions, Phys. Rev. C **90**, 017901 (2014).

[41] R.-q. Wang, J. Song, and F.-l. Shao, Yield correlations and p_T dependence of charm hadrons in Pb + Pb collisions at $\sqrt{s_{NN}} = 2.76$ TeV, Phys. Rev. C **91**, 014909 (2015).

[42] Q.-B. Xie and X.-M. Liu, Quark production rule in $e^+e^- \rightarrow$ two jets, Phys. Rev. D **38**, 2169 (1988).

[43] Q. Wang, Z.-G. Si, and Q.-B. Xie, Simple understanding of the energy dependence of the B/M ratio and hadron multiplicities in e + e-annihilation, Int. J. Mod. Phys. A **11**, 5203 (1996).

[44] F.-l. Shao, G.-j. Wang, R.-q. Wang, H.-h. Li, and J. Song, Yield ratios of identified hadrons in p+p, p+Pb, and Pb + Pb collisions at energies available at the CERN Large Hadron Collider, Phys. Rev. C **95**, 064911 (2017).

[45] C. Tsallis, Possible generalization of Boltzmann-Gibbs statistics, J. Stat. Phys. **52**, 479 (1988).

[46] V. Khachatryan et al. (CMS Collaboration), Strange particle production in pp collisions at $\sqrt{s} = 0.9$ and 7 TeV, J. High Energy Phys. 05 (2011) 064.

[47] T. Sjöstrand, S. Mrenna, and P. Z. Skands, PYTHIA 6.4 physics and manual, J. High Energy Phys. 05 (2006) 026.

[48] B. Andersson, G. Gustafson, G. Ingelman, and T. Sjöstrand, Parton fragmentation and string dynamics, Phys. Rep. **97**, 31 (1983).

[49] P. Z. Skands, Tuning Monte Carlo generators: The Perugia tunes, Phys. Rev. D **82**, 074018 (2010).

[50] N. Fischer and T. Sjöstrand, Thermodynamical string fragmentation, J. High Energy Phys. 01 (2017) 140.

[51] C. Bierlich and J. R. Christiansen, Effects of color reconnection on hadron flavor observables, Phys. Rev. D **92**, 094010 (2015),.

[52] B. R. Webber, A QCD Model for Jet Fragmentation Including Soft Gluon Interference, Nucl. Phys. **B238**, 492 (1984).

[53] P. Bartalini and L. Fano, eds., Proceedings, 1st International Workshop on Multiple Partonic Interactions at the LHC (MPI08) (DESY, Hamburg, 2009), arXiv:1003.4220.

[54] P. Z. Skands, in Proceedings, 1st International Workshop on Multiple Partonic Interactions at the LHC (MPI08) (DESY, Hamburg, 2009), pp. 284–297, arXiv:0905.3418.

[55] T. Sjöstrand, S. Mrenna, and P. Z. Skands, A brief introduction to PYTHIA 8.1, Comput. Phys. Commun. **178**, 852 (2008).

[56] B. I. Abelev et al. (STAR Collaboration), Identified Baryon and Meson Distributions at Large Transverse Momenta from Au + Au Collisions at s(NN) ∗ ∗(1/2) = 200-GeV, Phys. Rev. Lett. **97**, 152301 (2006).

[57] R. Derradi de Souza (ALICE Collaboration), Identified particle production in pp collisions at $\sqrt{s} = 7$ and 13 TeV measured with ALICE, J. Phys. Conf. Ser. **779**, 012071 (2017).

[58] N. Jacazio (ALICE Collaboration), Light flavor hadron production as a function of the charged-particle multiplicity at the LHC, Nuovo Cim. Soc. Ital. Fis. **40C**, 7 (2017).

[59] T. Sjöstrand, The development of MPI modelling in PYTHIA, arXiv:1706.02166.

[60] J. H. Chen, F. Jin, D. Gangadharan, X. Z. Cai, H. Z. Huang, and Y. G. Ma, Parton distributions at hadronization from bulk dense matter produced at RHIC, Phys. Rev. C **78**, 034907 (2008).

[61] E. M. Aitala et al. (E791 Collaboration), Asymmetries between the production of D^+ and D^- mesons from 500-GeV/c π^-—nucleon interactions as a function of x_F and p_t^2, Phys. Lett. B **371**, 157 (1996).

[62] E. M. Aitala et al. (E791 Collaboration), Asymmetries between the production of D_s^- and D_s^+ mesons from 500-Gev/c π^- nucleon interactions as functions of x(F) and $p - transverse^2$, Phys. Lett. B **411**, 230 (1997).

[63] E. Braaten, Y. Jia, and T. Mehen, The Leading Particle Effect from Heavy Quark Recombination, Phys. Rev. Lett. **89**, 122002 (2002).

[64] T. Pierog, I. Karpenko, J. M. Katzy, E. Yatsenko, and K. Werner, EPOS LHC: Test of collective hadronization with data measured at the CERN Large Hadron Collider, Phys. Rev. C **92**, 034906 (2015).